Understanding the classical maize floral development mutant, *Polytypic ear1*

By

Kimberly Rochelle Rispress

July 2023

Director of Thesis: Beth Thompson

Major Department: Biology

Abstract

Maize produces two inflorescences, the tassel and ear, which are critical for both plant reproduction and agriculture. The classical semi-dominant mutant, *Polytypic ear1* (*Pt1*), affects multiple aspects of inflorescence development, including floral development. *Pt1* heterozygote ears and tassels appear to have barren tips with extra floral organs towards the base with extra silks or branch-like protrusions. While the causative gene is unknown, RNA-seq provided direction for candidate gene analysis. Our top candidate gene, *ethylene response sensor1* (*ers1*), encodes a putative ethylene receptor that shows allele-specific expression in *Pt1*. Ethylene receptors negatively regulate ethylene signaling, and in *Arabidopsis*, dominant mutations confer ethylene insensitivity. I hypothesized that overexpression of ethylene receptors may also confer a similar ethylene insensitive phenotype. To test this hypothesis, I evaluated ethylene sensitivity of *Pt1* mutants. *Pt1*/+ siblings had no significant difference in growth in the presence and absence of the ethylene precursor ACC, but these results are not conclusive due to lack of robust wildtype results. While the *ers1* RNA *in situ* hybridization failed to detect *ers1* transcripts, the *in situs* of genes expressed in the boundary between upper and lower florets were similar in normal and *Pt1*/+ plants. The pectin localization patterns of *Pt1*/+ plants differed from normal siblings suggesting that floral meristem determinacy could be linked to changes in cell wall dynamics.

Understanding the classical maize floral development mutant, *Polytypic ear1*

A Thesis

Presented to the Faculty of the Biology Department

East Carolina University

In Partial Fulfillment of the Requirements for the Degree

Master of Science in Molecular Biology and Biotechnology

By

Kimberly Rispress

July 2023

Understanding the classical maize floral development mutant, Polytypic ear1

By

Kimberly Rochelle Rispress

APPROVED BY:

Director of Thesis

Beth Thompson, PhD

Committee Member

Lauren Anllo, PhD

Committee Member

Carol Goodwillie, PhD

Chair of the Department of Biology

David Chalcraft, PhD

Dean of the Graduate School

Kathleen Cox, PhD

TABLE OF CONTENTS

LIST OF TABLES

LIST OF FIGURES

Chapter 1: Introduction

Importance of maize flowers

Flowers are important for plant reproduction. Many grass flowers also provide food for humans and livestock. Maize is part of the angiosperm family due to the development of seeds within carpels covered by the ovary wall. Along with wheat and rice, maize is a part of the grass family with a distinct type of flower. The basic structural unit of grass inflorescences, the spikelet, contains an axillary branch with two bracts, called glumes, extending under grass-specific flowers. Maize is a monocot with female and male flowers, ears and tassels respectively, segregated to separate inflorescences of the same plant (Khan, 2017). Tassel size correlates with number of pollen grains, while maize ear size correlates with size and number of kernels (Li, Zhong, Yang, and Zhang, 2018). Inflorescence morphology directly impacts yield by determining the number and position of flowers.

Maize inflorescence development

All plant growth and development depend on meristems. Tassels arise from a meristem at the apex of the plant while ears arise from meristems in the axils of leaves. After development transitions from vegetative growth to reproductive, the vegetative meristems convert into inflorescence meristems, indeterminate meristems that make an undefined number of primordia (Bortiri, Jackson, and Hake, 2006). In tassels, inflorescence meristems initiate indeterminate branch meristems before initiating spikelet pair meristems, while ear inflorescence meristems directly initiate spikelet pair meristems ***(Figure 1)***. Determinate meristems, like spikelet pair meristems, are consumed after initiating a defined number of meristem or organ primordia.

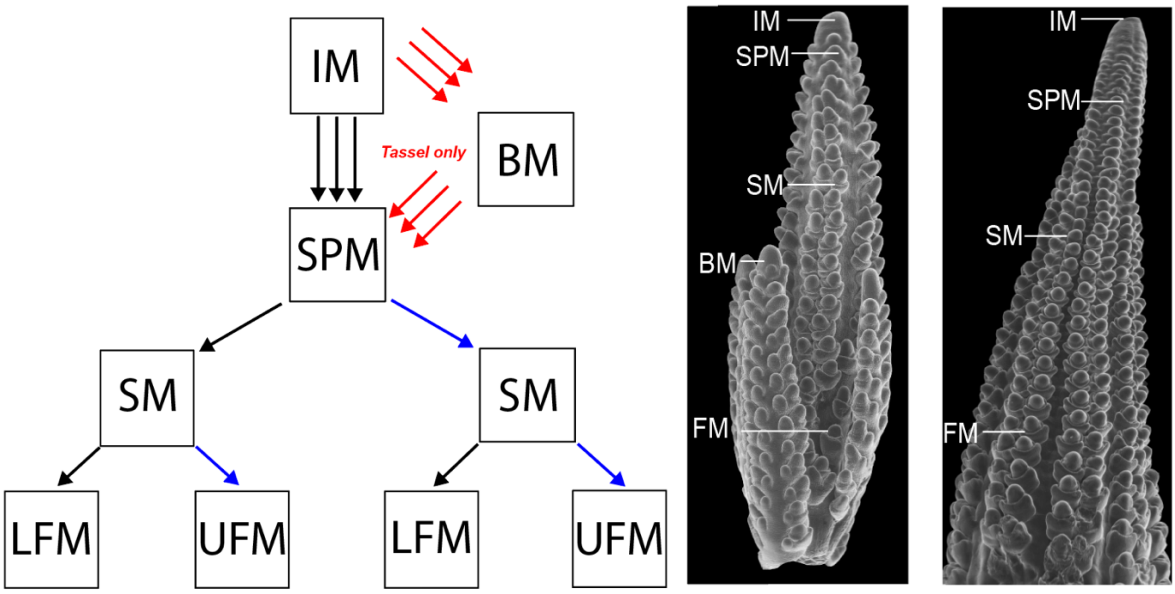

Figure 1: **Floral development in maize starts with meristems**. Indeterminate meristems (3 arrows) make an undefined number of organs. Inflorescence meristems (IM) initiate branch meristems (BM) in tassels only (red arrows). Next, spikelet pair meristems (SPM) are formed. Determinate meristems (1 arrow) are consumed after initiating a certain number of organs. Spikelet pair meristems initiates one spikelet meristem (SM) before converting (blue arrow) into a spikelet meristem. Each spikelet meristem initiates a lower floral meristem (FM) before converting into an upper floral meristem. (Images from Amoiroglou, 2019)

Spikelet pair meristems initiate a spikelet meristem before converting identity to another spikelet meristem. Finally, the spikelet meristems each initiate the lower floral meristem and convert identity to the upper floral meristem (Kaplinsky and Freeling, 2003; Yang et al., 2022).

Although their final appearance is quite different, the ear and tassel both develop most of the same floral organs (***Figure 2***). The upper and lower florets are enclosed in two bracts, called glumes. Long branches only develop at the base of tassels due to branch meristems (Tanaka, Pautler, Jackson, and Hirano, 2013). Grass florets have leaf-like floral organs called lemma and palea along with glandular-like lodicules that swell at anthesis (Bommert et al., 2005; Ambrose et al., 2000). In early floral development, all flowers have three stamen and three carpels. Sex determination occurs when stamens arrest in female spikelets and carpels abort via programmed cell death in male spikelets (Cheng, Greyson, and Walden, 1983). In ears, the lower floret aborts resulting in spikelets containing a single female floret, whereas in tassels, both florets develop resulting in spikelets containing two male florets.

Genetic regulation of maize floral development

MADS-box genes encode transcription factors that control floral development and floral organ identity in plants. While plant genomes have MADS-box genes that encode both MIKC-type transcription factors (type II) and non-MIKC-type transcription factors (type I), the latter do not control floral development (Gramzow and Theissen, 2010). The MIKC-type transcription factors have conserved MADS-box, intervening (I), Keratin-like, Carboxy-terminal (C) domains. The highly conserved MADS-box domain is involved in DNA binding and nuclear localization (Theißen, Kim, and Saedler, 1996). The I-domain also contributes to the specificity of protein dimerization (Riechmann et al., 1996). The K-domain is involved in formation of dimers and

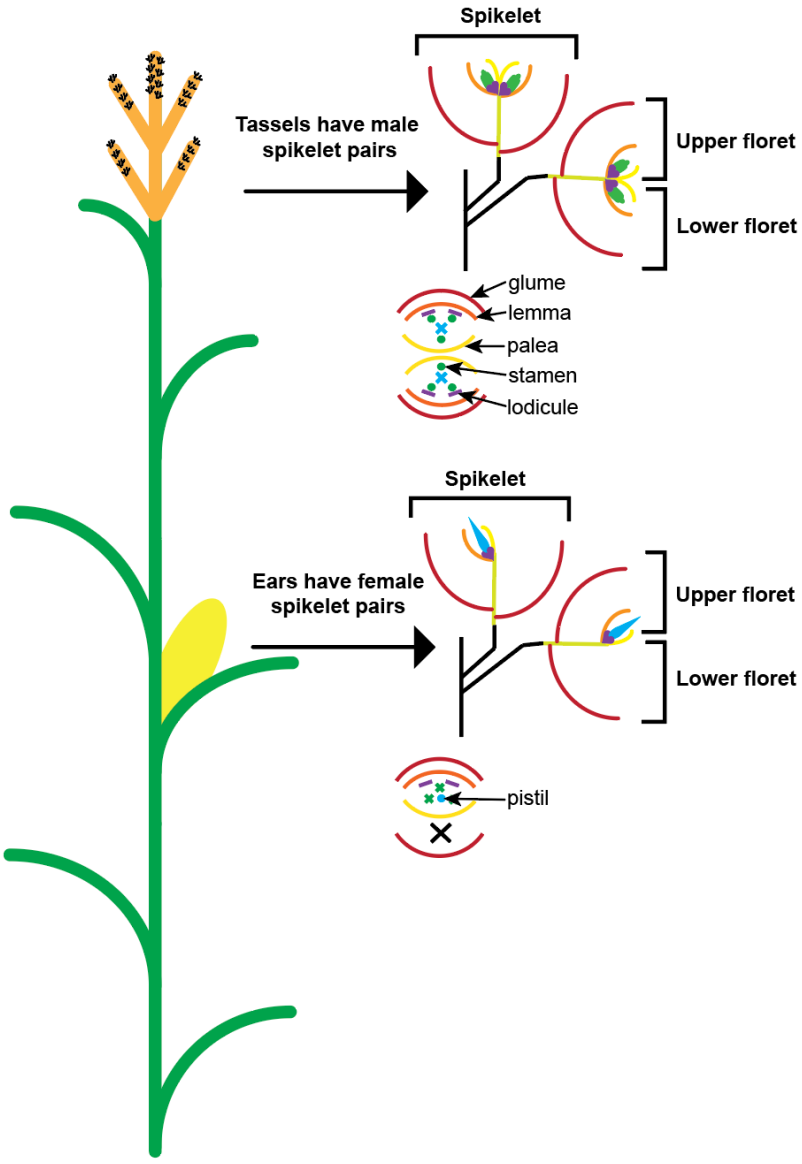

Figure 2: Male and female maize inflorescences share many common structures. Tassels (orange) grow at the apex of the plant, while ears (yellow) grow in the leaf axil. Glumes (red) enclose each spikelet. Each male floret (upper and lower) and each female upper floret are enclosed in lemma (orange) and palea (yellow) with two lodicules in between (purple). Male flowers have three stamens (green), while female flowers have one pistil (blue) formed from two fused carpels. The aborted lower floret in ears leaves one floret in mature ear spikelets.

multimers (Kaufmann, Melzer, and Theissen, 2005). The more variable C-domain protein contributes to tetramer formation and transcription activation (Theißen, Melzer, and Ruümpler, 2016). The MIKC-type proteins form dimers and tetramers to bind conserved DNA sequences called CArG-boxes (consensus sequence CC[A/T]$_6$GG). One dimer composed of two MADS-box proteins binds to a single CArG box. Two dimers bind to two CArG boxes to regulate transcription of downstream targets through either activation or repression (Gramzow and Theissen, 2010).

The most well-known example of MADS-box regulation of floral development is summarized by the ABC model, first identified in *Arabidopsis thaliana*. According to the model, there are different classes of floral organ identity genes in that work in combinatorial fashion to regulate expression of target genes and specify floral organ identity (***Figure 3***). The study of mutants with some or all floral organs replaced with organs of a different identity led to the development of the floral development model. First whorl sepals are specified by *APETALA1* (*AP1*) and *APETALA2* (*AP2*) which are A class genes (Alejandra Mandel et al., 1992; Jofuku et al., 1994). Class A and B genes specify petals, also known as second whorl organs. Class B genes include *APETALA3* (*AP3*) and *PISTILLATA* (*PI*). The third whorl stamens are specified by B and C class genes, while carpels are specified by class C gene *AGAMOUS* (*AG*) in the fourth whorl (Jack et al., 1992; Goto and Meyerowitz, 1994; Yanofsky et al., 1990). The fifth whorl ovule gene is up for debate, but some researchers believe *SEEDSTICK* (*STK*) specifies ovule development (Favaro et al., 2003). Class E genes, *SEPALLATA1/2/3/4* (*SEP1/2/3/4*), are required for floral organ identity in all four whorls (Becker and Theißen, 2003). All ABC genes are MIKC MADS-box genes except for *APETALA2*.

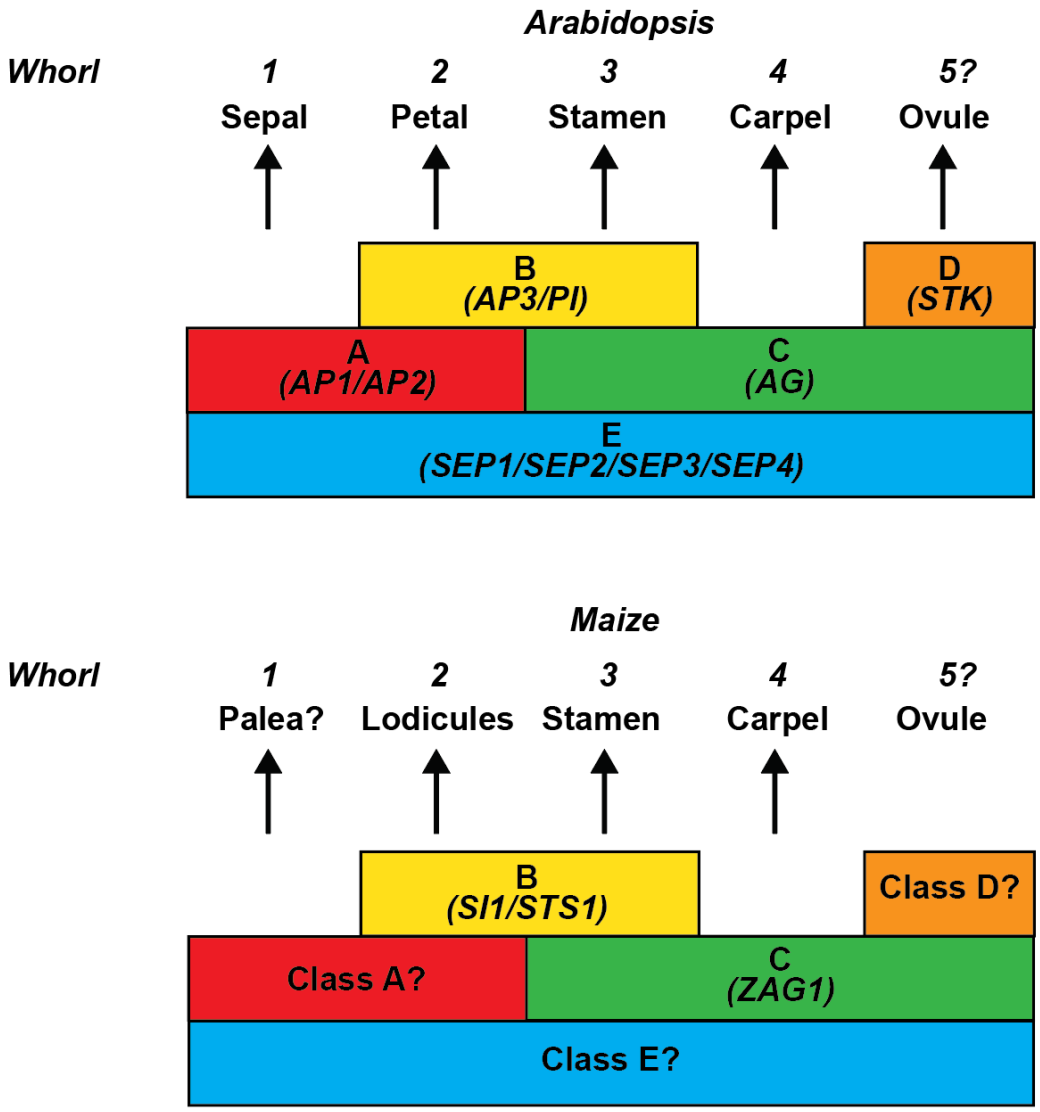

Figure 3: **The floral development model connects genes to floral structures.** (Top) In Arabidopsis, class A genes specify sepals. Petals are controlled by class A and B genes. Stamens are controlled by class B and C genes. Carpels are specified by class C genes. Class E genes also function to control all floral organs. Class D genes are up for debate, but some researchers believe they specify ovule development. (Bottom) In maize, class B genes are conserved to regulate lodicule and stamen growth. Class C genes are partly conserved to specify stamen and carpel growth.

In maize, class B genes seem to be conserved while class C genes are partly conserved (Li and Liu, 2017). *Sterile tassel silky ear1* (*sts1*) is a PI homolog that helps positively regulate maize B class genes as shown by homeotic conversion of stamens to carpels and lodicules to lemma-like organs in ears. *Sts1* mutants have lost *Zea mays MADS-box gene 16* (*Zmm16*) function (*PI/GLO-like* gene) (Bartlett et al., 2015). *Silky1* (*Si1*), an AP3 ortholog, is a male sterile mutant that has homeotic conversion of stamens to carpels and lodicules into palea/lemma-like structures just like *sts1* (Ambrose et al., 2000; Bartlett et al., 2015). STS1 forms heterodimers with SI1to bind DNA and regulate their own transcription (Whipple et al., 2004). *Zea agamous1* (*zag1*) is a class C MADS-box gene that is required for floral meristem determinacy as shown by indeterminate phenotypes in the fourth whorl (Mena et al., 1996). Another MADS-box gene, *bearded ear* (*bde*), is required to specify organ number and fate in the upper floret and floral meristem identity in the lower floret. BDE physically interacts with ZAG1 to regulate floral meristem fate and is in a sister-clade with class E genes (Thompson et al., 2009).

There are several other non-MADS-box genes involved in key stages of maize floral development that were found via mutant analysis. *Zea floricaula/leafy* (*zfl*) mutants have defects in floral determinacy, organ identity, and phyllotaxy. *zfl* coordinates the transition from vegetative to reproductive growth, influences inflorescence meristem size and organization, and promotes inflorescence branching (Bomblies et al., 2003). Like *zfl*, *droopyleaf1*(*drl1*) and *drl2* affects floral determinacy in maize (Strable and Vollbrecht, 2019). Floral organ identity and floral meristem determinacy are affected by *Silky3 (Si3)*, specifically in the stamen whorl (Luo et al., 2020).

Classic floral development mutant Polytypic ear1

The *Polytypic ear1 (Pt1)* is a classical developmental mutant that has severe floral defects with a semi-dominant inheritance pattern (Nelson and Postlethwait, 1954; Amoiroglou, 2019). The *Pt1* phenotype was first reported in 1954 when the mutation spontaneously arose in an unknown genetic background. *Pt1/+* plants have excess growth of the pistillate spikelet or an abnormally elongated ear axis with little or development of pistillate spikelets. Genetic modifiers may suppress the severity of the homozygote genotype causing the appearance of the heterozygote phenotype based on deviation from expected phenotypic ratios in controlled crosses (Nelson and Postlethwait, 1954; Amoiroglou, 2019). In early development, *Pt1* plants have abnormal branch meristems, spikelet meristems, glume primordia, and pistil primordia (Postlethwait and Nelson, 1964). The causative gene and underlying developmental effects of *Pt1* are unknown.

Previous work has characterized the *Pt1* phenotype in multiple defined inbred backgrounds, including A619, B73 and Mo17 lines (Amoiroglou, 2019). Compared to normal siblings, *Pt1* heterozygous (*Pt1/+*) ears and tassels appear to have barren tips (***Figure 4***). Florets often contain abnormal floral organs with branch-like protrusions. *Pt1*/+ tassels produce less pollen and some ectopic silks compared to normal siblings, while *Pt1* /+ ears can produce extra silks protruding from several ovules. *Pt1*/A619 tassels mostly resemble normal tassels with a few ectopic silks protruding from the florets. *Pt1*/B73 tassels can produce some short silks, while *Pt1*/Mo17 tassels have longer silks and some barren tips of branches. *Pt1*/+ ears usually produce extra silks at the bottom resulting from ovules producing more than one silk. *Pt1*/+ ears can also have barren patches at the top. *Pt1/B73* and *Pt1/Mo17* ears are similar, with a barren tip and indeterminate florets that produce extra florets and branch-like organs at the base. *Pt1*/A619 ears

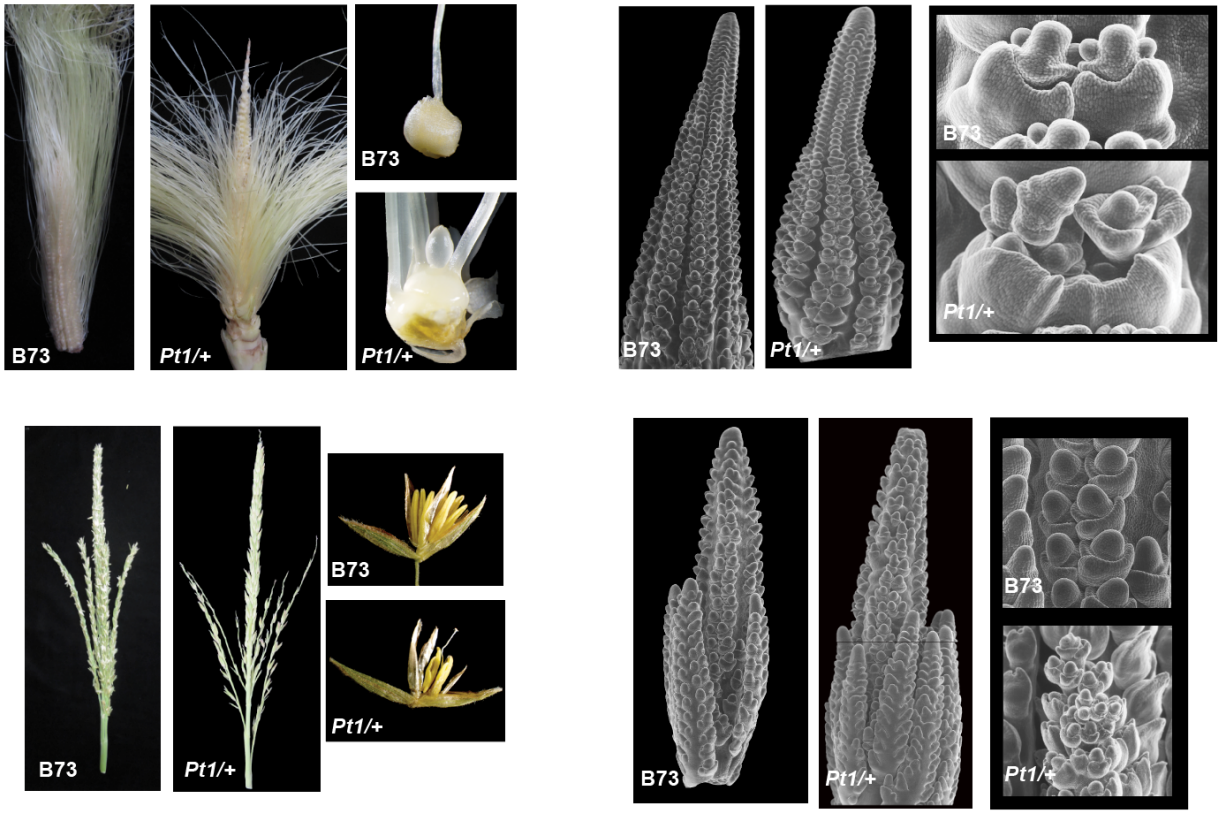

Figure 4: *Polytypic ear1* has severe floral defects. (Top row) Normal ears have well organized rows of kernels, each with one silk protruding from the ovule. *Pt1/+* ears often have barren patches at the top due to arrested growth. At the base, *Pt1/+* ovules have extra silks or abnormal branch-like organs protruding from them. (Bottom row) Tassels have male spikelet pairs along the main spike and branches. *Pt1/+* tassels can appear to have barren tips with a variable number of floral organs. Pt1/+ tassels often have indeterminate floral meristems. (Images from Amoiroglou, 2019)

mostly look like normal ears but some ovules at the base have extra silks and nucelli protruding from florets (Amoiroglou, 2019). In the B73 and Mo17 inbred backgrounds, the *Pt1*/+ phenotype is fully penetrant, but the severity of the *Pt1*/+ phenotype is variable. In contrast, in the A619 inbred background, *Pt1*/+ has a more variable phenotype while the *Pt1* homozygotes are still fully penetrant.

Interestingly, *Pt1* appears to have roles in both promoting and repressing meristem activity. Inflorescence primordia in *Pt1*/+ individuals often have fasciated inflorescence meristems and other meristems (i.e. spikelet pair, spikelet, and floral meristems) are indeterminate, consistent with increased meristem activity. However, spikelet pair meristems often arrest and develop derepressed bracts in *Pt1*/+ inflorescences (Amoiroglou, 2019). In some genetic backgrounds, *Pt1/Pt1* inflorescences almost completely lack lateral primordia, suggesting reduced meristem activity. Therefore, *Pt1* seems to affect spikelet pair meristem maintenance and determinacy in spikelet meristems and floral meristems.

Rough mapping results found that the *Pt1* gene was located on chromosome 6 bin 5 (Postlethwait and Nelson, 1964), but the gene responsible for the *Pt1* mutant phenotype is unknown. To search for the causative gene in *Pt1* mutants, we used a positional cloning approach to define an increasingly narrower interval in the genome until the molecular lesion causing the mutant phenotype has been found (Gallivotti and Whipple, 2015). Other floral development mutant maize genes such as *Silky3*, *bearded ear*, and *sterile tassel silky ear1* have been identified in the DNA coding sequence using map-based cloning (Luo et al., 2020; Thompson et al., 2009; Bartlett et al., 2015). Mapping populations are created from two parents with different genetic backgrounds that are crossed at least twice to allow recombination to occur. The recombinant chromosomes are used to map the genetic loci causing the mutant

phenotype to a particular place in the genome. *Pt1* segregating families were backcrossed twice to A632 inbred (***Figure 5***). *Pt1*/+ plants were backcrossed with A632 inbreds to create the F1 population. The F1 offspring (*Pt1*/A632) were backcrossed with parental A632 inbreds to create the F2 populations. Populations that have been further introgressed may also be suitable for mapping. PCR-based genotyping allowed the *Pt1*-containing interval to be narrowed down to a 5.3 Mb region on chromosome 6 bin 5 between SSR markers *phi129* and *umc1352a* (Amoiroglou, 2019).

The *Pt1* phenotype could be caused by a change in the amino acid sequence, resulting in altered protein function, or a change in RNA levels. RNA-sequencing can detect both a change in RNA levels and a change in mRNA sequence that is predicted to change the amino acid sequence. Within the *Pt1*-containing interval, there are 111 expressed genes. We looked for changes in the RNA sequence that were also predicted to change the protein sequence. Within the *Pt1*-containing interval, 112 variants were predicted to have a high or moderate effect on protein function (Amoiroglou, 2019). However, all high/moderate effect SNPs are represented in the wildtype alleles found in the maize HapMap and thus unlikely to cause the *Pt1* phenotype. There were also 290 low effect SNPs, but these have not been investigated yet (Amoiroglou, 2019).

RNA-seq can also detect changes in RNA levels between two samples. Differential expression (DE) analysis finds changes in RNA expression levels by comparing the number of normalized reads aligned with certain transcripts. If the *Pt1* mutation is due to a change in regulatory DNA that leads to a difference in transcriptional levels, we expect to see the *Pt1* allele differentially expressed relative to the normal allele, also known as allele-specific expression. To test for allele-specific expression, there must be at least one polymorphism present in the RNA.

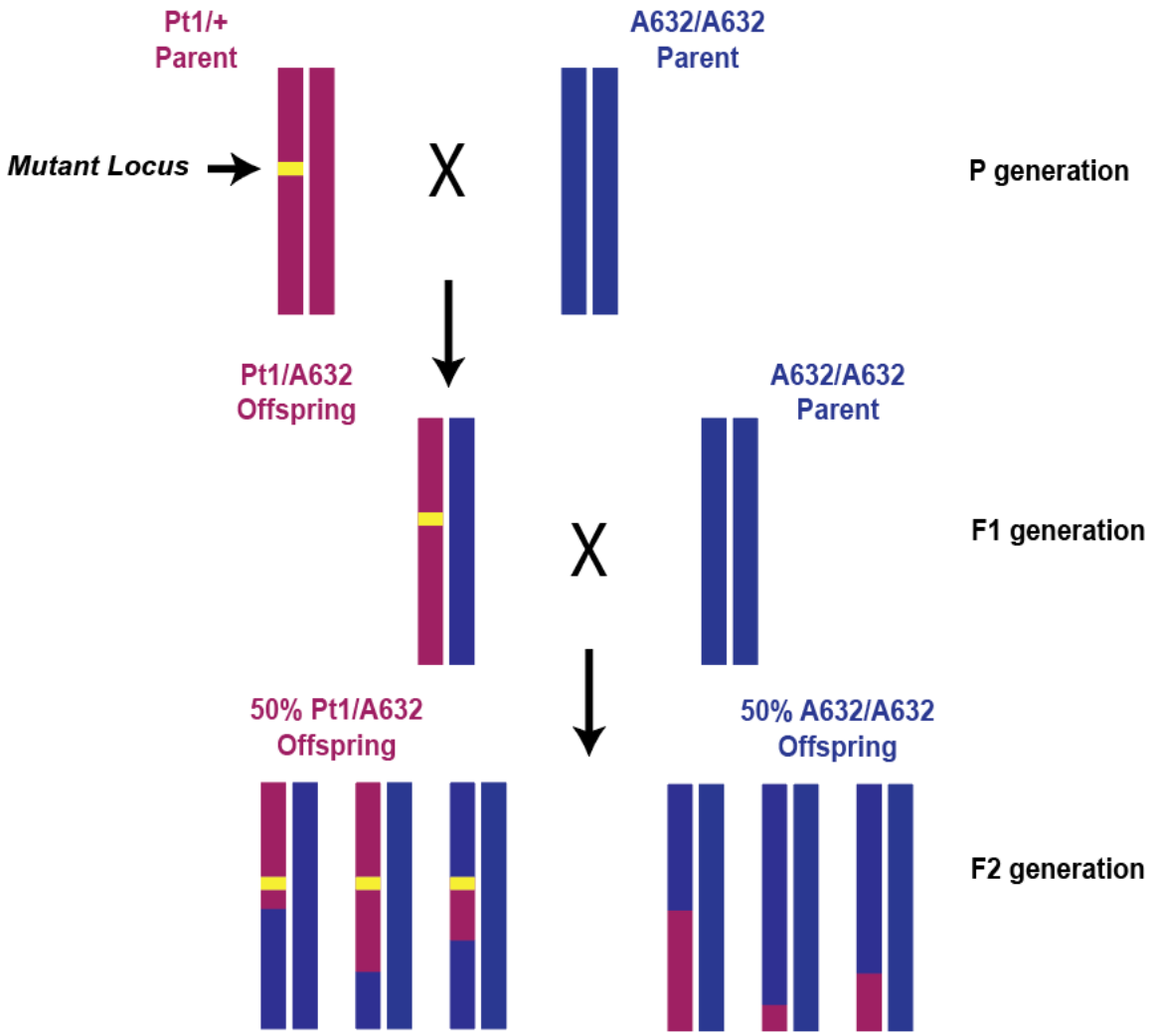

Figure 5: F2 backcross mapping populations. *Pt1* heterozygotes (maroon) segregating 1:1 in an unknown genetic background were crossed with A632 individuals (navy) to create the F1 population. The *Pt1*/A632 offspring from F1 were backcrossed again to the A632 parent to create the F2 population which will provide recombinant chromosomes for mapping purposes.

Of the 111 genes expressed in the *Pt1*-containing interval, six were downregulated and three were upregulated in *Pt1* mutants (***Table 1***; Amoiroglou, 2019). Three of the differentially expressed genes did contain polymorphisms in the RNA coding region. Of the six downregulated genes, only one, *zag1* which has already been characterized, has allele-specific expression. Yet two of the three upregulated genes have allele-specific expression. In *Pt1* mutants, class B and C genes are significantly downregulated compared to B73 plants which is consistent with the *Pt1* phenotype.

Pt1 is likely a gain-of-function mutation due to its semi-dominant inheritance pattern; therefore, I focused on one of the three upregulated genes as a candidate gene. Specifically, I focused on *ethylene response sensor1* (*ers1),* which encodes an ethylene receptor. Strikingly, *ers1* exhibits allele-specific expression with ~80% of the transcript in *Pt1/+* plants originating from the mutant chromosome. Also, *Pt1* ears share an ear phenotype with ethylene insensitive mutants making *ers1* our top candidate gene (J. Strable, personal communication).

In the absence of ethylene, ethylene receptors are active, which promotes degradation of ethylene transcription factors, ETHYLENE INSENSITIVE (EIN) and ETHYLENE INSENSITIVE-LIKE (EIL, ***Figure 6***). Ethylene response genes are not transcribed. When ethylene binds to an ethylene receptor such as ERS1, ethylene inhibits the receptors and decreases downstream inhibition of transcription factors leading to ethylene responses (Binder, 2020). In Arabidopsis, dominant mutations of *ers1* confer ethylene insensitivity (Liu and Wen, 2012).

To investigate if upregulation of *ers1* results in the *Pt1* phenotype, I carried out ethylene sensitivity assays and created tools to examine *ers1* expression in situ. I further investigated the *Pt1* phenotype by characterizing the boundary between the upper and lower florets by staining

Table 1: **Differentially expressed genes within the *Pt1*-containing interval** – Of the 111 expressed genes in the *Pt1*-containing interval, three were upregulated and six were downregulated (Amoiroglou, 2019).

Gene ID	Log(2) FC	Common name/homolog	Allele specific expression
Zm00001d037604	+2.63903226	Ethylene response sensor1	20% ref allele (G); 80% alt allele (A) only in mutants
Zm00001d037650	+6.84647504	Putative disease resistant protein	No SNPs
Zm00001d037751	+3.00369697	(LEA) hydroxyproline-rich glycoprotein family	30% ref allele (T); 70% alt allele (G) across mutants and normals
Zm00001d037565	-3.19701574	gibberellin 2-oxidase1	None
Zm00001d037609	-2.7393924	GDSL esterase/lipase	None
Zm00001d037623	-2.79794362	Rotundifolia-like 12	No SNPs
Zm00001d037651	-2.33488376	Subtilisin-like serine endopeptidase family protein	None
Zm00001d037672	-2.71905912	Putative leucine-rich repeat receptor protein kinase family protein	No SNPs
Zm00001d037737	-12.1538179	Zea AGAMOUS homolog1	35% ref allele (C); 65% alt allele (G) across mutants and normals

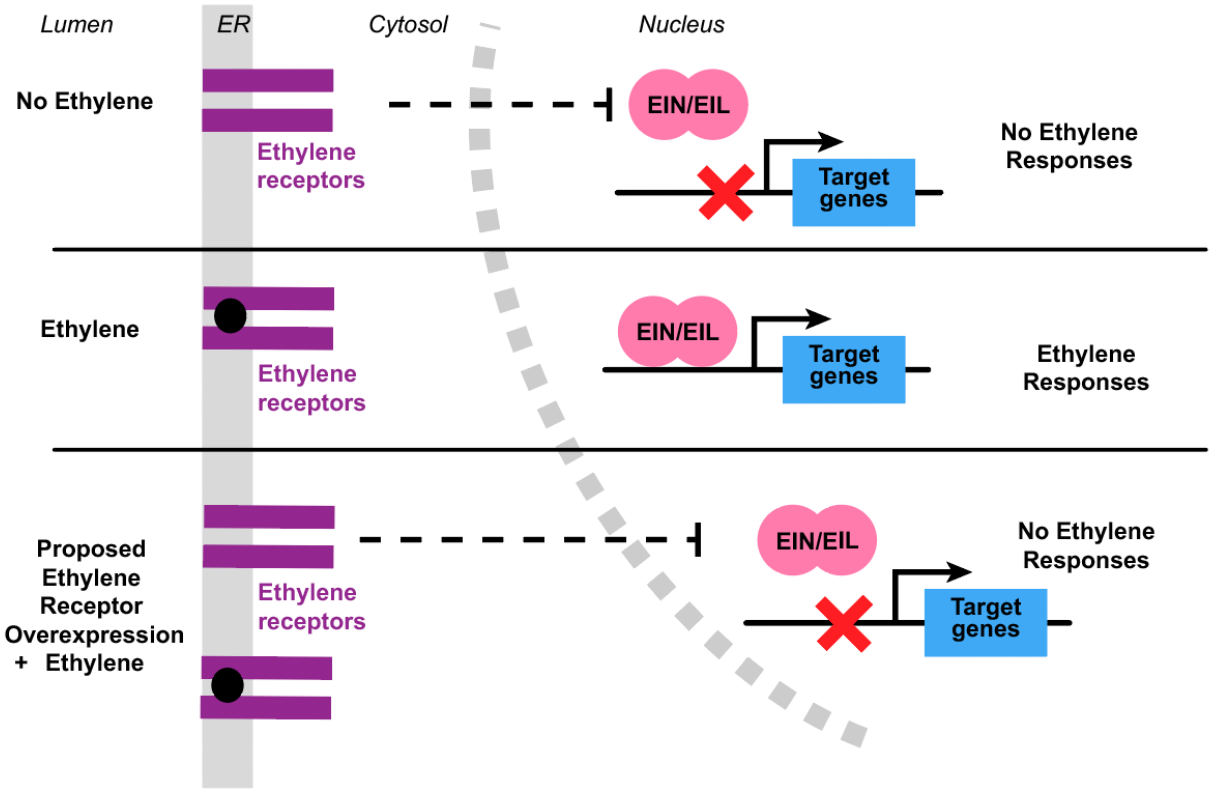

Figure 6 Ethylene signaling in maize. Ethylene receptors such as ERS1 negatively regulate ethylene signaling. (Top) In the absence of ethylene, the receptor is active, ethylene transcription factors are degraded, and ethylene response genes are not transcribed. (Middle) In the presence of ethylene, the receptor is inactivated, ethylene transcription factors are stabilized, and ethylene response genes are transcribed. (Bottom) I propose that overexpressing ethylene receptors could lead to ethylene insensitivity. If ethylene is unable to saturate the receptors, some receptors will always be active leading to no ethylene responses **(**Modified from Caren Chang, 2016)

with antibodies that recognize cell wall components that have distinct patterns during floral development. Studying *Pt1* will give us a better understanding of plant growth and development and provide insights into traits that impact yield.

Chapter 2: Methods

ACC Germination Assay

The 1-Aminocyclopropane-1-carboxylic Acid (ACC) germination assay was performed to test the ethylene sensitivity of *Pt1*/+ plants as described previously (Draves et al., 2022) with the following modifications. The positive control group was inbred W22 kernels, while the experimental group were kernels from two ears from *Pt1* families backcrossed to B73 five times segregating *Pt1* heterozygotes to normal siblings 1:1. Kernels were put in a 50 ml conical tube and soaked in water for 2 h while rotating. After replacing water with 6% bleach solution (3 ml 7.5% bleach diluted in 47 ml water), the kernels were washed with ddH2O five times. Stacks of three germination papers (Anchor Paper Company) were soaked in Captan solution (Bonide; 2.55 g in 1 L of millQ water), arranged landscape style on the lab bench, and 10 kernels were evenly spaced on the middle sheet. The germination papers were rolled from the left short edge to the right short edge and placed in 600 ml 0.5x LS media with or without 50 or 150 uM ACC (Sigma-Aldrich, 149101-M) and germinated in a dark incubator at 25°C. (Previous unsuccessful assays used a bad batch of ACC from Sigma-Aldrich, A3903). Media levels were checked daily and refilled to ensure germination papers remained saturated. Once shoots extended past the top of the roll, seedlings were removed from the incubator (approximately 7 d after planting). The primary root, mesocotyl, coleoptile, and shoot lengths were measured for each seedling (***Figure 7***).

Plant Growth and Tissue Fixation

To characterize the boundary between upper and lower florets in *Pt1* plants, plants were grown in the greenhouse on a 12h light, 12h dark schedule. *Pt1* was backcrossed to B73 at least four

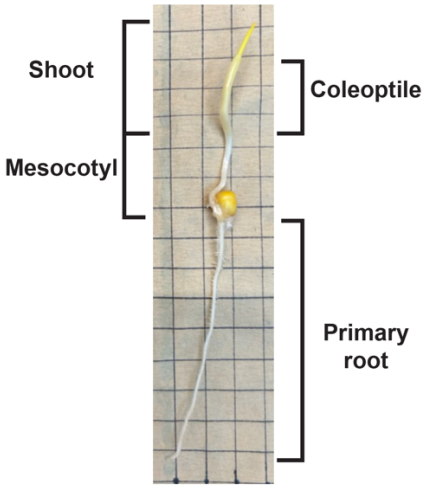

Figure 7: ACC Germination Assay Measurements. The primary root, mesocotyl, coleoptile, and shoot were measured for each seedling. The primary root is often the longest root extending beneath the seed with lateral roots extending from it. The mesocotyl is a white embryonic stem that extends from the seed to the coleoptile. The coleoptile is a clear embryonic leaf that often encloses the shoot (which is often yellow when grown in the dark due to the absence of sunlight).

times. Recombinant individuals with different genotypes at the SSR markers bnlg1922 and umc1352a were excluded due to ambiguous genotypes. Fourteen-day old seedlings were transplanted into 3- or 2-gallon pots in groups of three or two, respectively. *Pt1/+* and B73 ear primordia (1 cm) were dissected ~8 weeks after planting and fixed overnight at 4°C in formalin-acetic acid-alcohol (FAA). Samples were dehydrated through a graded ethanol series (70%, 85%, 95%, 100%) each hour, with two changes in 100% ethanol (the last included eosin incubated overnight at 4°C). Samples were passed through a graded Histoclear series (0:1, 1:1; ethanol:Histoclear) at room temperature with three changes in 100% Histoclear; all changes were 1 h each with the last incubation including Paraplast X-tra wax chips (Leica) overnight. The samples were put in a 60°C oven to melt the wax. The first day included three wax changes every 3 h. Over the next two days, the wax was changed two times daily with at least 4 h between each change. On the third day, the wax was changed once. After the wax was melted, the samples were poured into aluminum tins and arranged equidistant before cooling. Embedded ears were stored at 4°C until sectioning. *Pt1/+* and normal sibling ears were sectioned longitudinally into 10 µm sections on a Microm HM315 Microtome before mounting on ProbeOn Plus slides (Fisher Scientific).

Genotyping

To differentiate between normal and *Pt1/+* individuals, plants were genotyped using SSR markers that flank the *Pt1*-containing interval, bnlg1922 and umc1352a (**Table 2**). DNA was extracted from leaf tissue using a basic miniprep protocol. PCR reactions were done using the reaction components for the Taq PCR protocol listed in ***Table 3*** using the thermocycler conditions listed in ***Table 4***. PCR products were run on a 3.5% Metaphor agarose gel. The

Table 2: PCR primers – The first two primer sets were used to genotype all plants. The next two primer sets were gene-specific primers used to make the RNA fragments for the RNA *in situ* probes. To check for the correct orientation of the plasmid, the T7 primer was used with the ers1-3 forward primer. The final primer was used to amplify the piece of the plasmid needed for in vitro transcription.

Primer	Primer Sequences
umc1352a	5'-GTGACGAGATGGTGCAGAAAGAT-3' 5'-CCTGGAGGTGGAAGGAGAGG-3'
bnlg1922	5'-GTCTTGGGCAGTAATCAGGC-3' 5'-TCGATCAAAGACGTTCATGC-3'
Ers1-3	5'-GCCCGTGATCTGCTATTGGA-3' 5'-TTCGCTTTCCAGCCAGATGT-3'
Ers1-4	5'- ATGCTTCCTCCAGACAGTGC-3' 5'- TGGATGCAAGTCAAGAGCGT-3
T7	5'-TAA TAC GAC TCA CTA TAG GG-3'
M13	(-24) 5'-CGCCAGGGTTTTCCCAGTCACGAC-3' (-17) 5'-CAGGAAACAGCTATGAC-3'

Table 3: **PCR components** – All PCR reactions used the Flexi Go-Taq PCR components (Promega). PCR was used to genotype normal and Pt1/+ siblings. Taq Touchdown PCR amplified ers1 fragments. Taq Touchdown Colony PCR was used to check the orientation of the sequence in the cloning vector. M13 PCR amplified the extracted plasmid prior to invitro transcription.

Component	**Taq and Taq Touchdown Colony**	**Taq Touchdown**	**M13**
Template	1 µl	2 µl	3 µl
BBL water	10.9 µl	21.75 µl	19.5 µl
25 mM $MgCl_2$	2.5 µl	5 µl	5 µl
DMSO	1 µl	2 µl	2 µl
10 µM F primer	1 µl	2 µl	2.5 µl
10 µM R primer	1 µl	2 µl	2.5 µl
2 mM dNTPs	2.5 µl	5 µl	5 µl
5x Flexitaq buffer	5 µl	10 µl	10 µl
Flexi Go-Taq (5 u/µl)	0.1 µl	0.25 µl	0.5 µl
Total reaction volume	**25 µl**	**50 µl**	**50 µl**

Table 4: Thermocycler conditions for PCR -). The Taq reaction was used to genotype normal and Pt1/+ siblings. Taq Touchdown reaction amplified ers1 fragments. Taq Touchdown Colony reaction to check the orientation of the sequence in the cloning vector. M13 PCR amplified the extracted plasmid prior to invitro transcription.

PCR Program	Taq	Taq Touchdown	Taq Touchdown Colony	M13
Thermocycler conditions	97°C – 3 min [95°C – 30 s 55°C – 30 s 72°C – 30 s] 35 cycles 72°C – 5 min	95°C – 1 min [95°C – 30 s 62°C* – 30 s 72°C – 70 s] 9 cycles *(annealing temp decreases by 1°C every cycle) [95°C – 30 s 53°C – 30 s 72°C – 50 s] 33 cycles 72°C – 7 min	95°C – 5 min [95°C – 30 s 62°C – 30 s 72°C – 70 s] 9 cycles [95°C – 30 s 53°C – 30 s 72°C – 50 s] 33 cycles 72°C – 7 min	95°C – 1 min [95°C – 30 s 55°C – 30 s 72°C – 50 s] 35 cycles 72°C – 5 min

normal siblings had a top band only for both markers, while the *Pt1/+* siblings had a top and bottom band for both markers (***Figure 8***). Recombinant plants had a homozygous wildtype genotype at one marker and a heterozygous *Pt1* genotype at the other marker. Recombinants were excluded from the results due to unclear genotype at the *Pt1* locus.

RNA Extraction

To create *ers1*-specific RNA probes to examine *ers1* expression *in situ*, two B73 shoot apices were dissected from 10-day old seedlings, flash frozen in liquid nitrogen, and stored at -80°C. Under the fume hood, frozen tissue was ground in 500 µl Trizol (Invitrogen) with a pestle, vortexed for 30 s, incubated at room temperature for 5 min, followed by the addition of 100 µl chloroform, vortexed for 30 s, and incubated at room temperature for 2-3 min. The tissue was centrifuged at 4°C for 15 min at maximum speed (16,110 rcf). The aqueous layer (top) was transferred to a new tube and an equal amount of chloroform was added. After vortexing for 30 s, the tube sat on ice for 5 min before centrifuging for 15 min at 4°C. Any solution added to the sample after this was kept on ice. The aqueous layer was removed and put in a new tube with 1/10th volume 3M sodium acetate and an equal volume of isopropanol. After mixing by inverting several times, the tube was incubated on ice for at least 20 min. The sample was centrifuged at 4°C for 15 min to precipitate RNA. The supernatant was discarded and the pellet was washed in 500 µl 70% EtOH. After sitting for 5 min on ice, the sample was centrifuged at max speed for 10 min at 4°C. The EtOH was removed, and the pellet was allowed to air dry on ice for 15 min. The pellet was resuspended in 25 µl RNase-free water and 0.5 µl RNasin Plus (Promega). To assess RNA integrity, one µl RNA was visualized on a 1% agarose gel with 5 µl RNase-free water and 1 µl 6x loading dye. Two distinct bands for the two ribosomal subunits

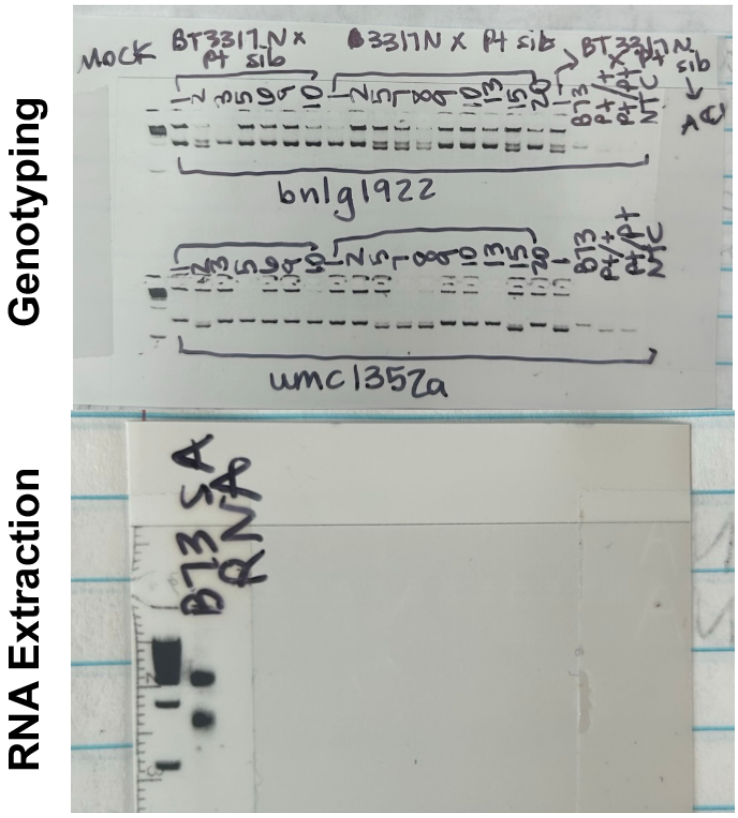

Figure 8: Gels for genotyping and evaluating RNA extraction – The top gel shows genotyping results for normal and *Pt1/+* siblings. The top band for both SSR markers, bnlg1922 and umc1352a, shows a normal genotype while two bands show a *Pt1/+* genotype. The middle gel shows that the extracted RNA is intact as evidenced by the two distinct bands (ribosomal subunits). The bottom gel shows that the RNA probes were hydrolyzed.

showed the RNA was not degraded (***Figure 8***). RNA concentration (ng/µl) was measured using the NanoDrop One Spectrophotometer. A260/280 value close to two was considered a good RNA sample.

RNA Probe Design and Production

Two sets of *ers1*-specific PCR probes were designed to target different regions within the coding sequence near the 3' end. The first set included the coding sequence, while the second set included some of the 3' UTR with the coding sequence. To make cDNA, reverse transcription was performed according to manufacturer's instructions including first heating 1 µL 50 µM oligodT primer (Superscript III first-strand synthesis system for RT-PCR; Invitrogen) and 5 µg of B73 RNA obtained from shoot apices at 65°C for 5 min. After sitting on ice for at least 1 min, the cDNA synthesis mix was added including 1 µL SuperScript III reverse transcriptase (200 U/µl). The reverse transcription reaction was incubated at 55°C for 50 min and terminated at 85°C for 5 min. After chilling on ice, the cDNA was centrifuged before adding 1 µl RNase H (2 units/µl). The cDNA was incubated for 20 min at 37°C. The cDNA was diluted 1:1 with ddH_2O and stored at 4°C. A 759 bp fragment of the cDNA was amplified via PCR using the first set of *ers1*-specific primers successfully, while the second set of ers1-specific primers failed to amplify the 672 bp fragment (sequences in ***Table 2***). The Taq Touchdown PCR reaction used the components listed in ***Table 3*** with the thermocycler conditions listed in ***Table 4***.

PCR products were purified with the AccuPrep PCR Purification kit (Bioneer) according to manufacturer's instructions. Nine ng purified ers1 fragment was ligated into the 50 ng pGEM-T easy vector (Promega) with 3 units/µl T4 DNA ligase incubated overnight at 4°C. Stellar competent cells (TakaraBio) were thawed and 50 µl were transferred into a 14 ml falcon tube.

After adding 2 µl ligation product, the tube was incubated on ice for 30 min. The cells were put in a 42°C water bath for 45 s before returning to ice for 2 min. SOC medium was added to the tube (448 µl) and the cells were incubated by shaking (160-225 rpm) for 1 h at 37°C. Two LB + ampicillin plates (100 mg/ml) were prepped with 40 µl x-gal in DMSO (20 /ml) and 7 µl IPTG (200 ng/ml). One plate received 100 µl of the cell mixture while the other plate got 400 µl. The plates were incubated overnight at 37°C. After the vector was transformed into E coli, several white colonies were each added to 50 µl BBL water. Colony PCR was performed using the T7 promoter and *ers1-3* forward primer (***Table 2-4*****)** to ensure the insert was in the correct orientation to amplify the antisense strand. To isolate a single colony, the colony was streaked on another LB + ampicillin plate (100 mg/ml) and colony PCR was repeated to check the purity of the plasmid. The colony was grown in 3 ml LB broth (+ 3 µl 100 mg/ml ampicillin) and incubated overnight at 37°C.

The plasmid was extracted from the colony using the Plasmid Mini Extraction kit (Bioneer) according to manufacturer's instructions. The extracted plasmid was amplified using M13 forward and reverse primers (***Tables 2-4***). M13 PCR products (obtained from Dr. Hailong Yang) for Bowman-Birk-type inhibitor *(BBTI), pectate lyase* homolog, and *arginine decarboxylase1* (*adc1*) were also amplified (GRMZM2G114552; GRMZM2G131912; GRMZM2G396553; Yang et al., 2022).

To synthesize anti-sense RNA probes, in vitro transcription was performed according to manufacturer's instructions including 10 µl M13 PCR product, 1 µl T7 RNA polymerase (Promega), and 2 µl DIG RNA labeling mix (Roche Diagnostics) and incubated overnight at 37°C. The next day, 1 ul (2000 U/ml) DNaseI was added to in vitro transcription products and incubated at 37°C for 20 min. To precipitate probe, 2.5 µl 3M NaOAc, 75 µl 100% EtOH, and 1

µl 10 mg/ml yeast tRNA was added and incubated at -20°C overnight. The mixture was spun at max speed at 4°C for 30 min before removing the supernatant. The pellet was washed with 70% EtOH. The pellet was re-spun for 10 min and the EtOH was removed. After air drying the pellet on ice for 10 min, the pellet was resuspended in 50 µl nuclease-free water. Carbonate hydrolysis reduced the length of the RNA probe to 150 bp to allow entry into the cell using the formula below (under ***Table 5***). Fifty µl 2x CO_3^- buffer was added to the probe and put in a 60°C heat block for the calculated length of time in minutes (***Table 5***). The overnight precipitation was repeated. After removing EtOH, the pellet was resuspended in 50 µl 50% formamide and stored at -80°C.

RNA in situ hybridization

To investigate the boundary between upper and lower florets and examine *ers1* expression, RNA *in situ* hybridization was performed as described previously (Yang et al., 2022) and briefly summarized below. The sections were dewaxed with Histoclear twice for 10 min each. The sections were rehydrated with a graded EtOH series for 90 s each (100%, 100%, 95%, 90%, 80%, 70%, 50%, 30% - 90% and below have 5 ml 8.5% NaCl) followed by 0.85% NaCl. Pronase digestion was performed for 25 min at 37°C (47 ml DEPC water, 2.5 ml Tris pH 7.5, 0.5 ml EDTA, and 157 µl 40 mg/ml pronase) followed by a 2-minute 0.2% glycine treatment (0.1 g glycine dissolved in 50 ml 1xPBS). Slides were refixed with 3.7% formaldehyde (5 ml 37% formaldehyde, 45 ml 1x PBS) for 10 min under the fume hood followed by a 2-minute 1xPBS wash. The slides were treated with acetic anhydride treatment for 10 min (slides in 0.1M triethanolamine solution plus 3 mL acetic anhydride), followed by

Table 5: Calculated times for carbonate hydrolysis (using the formula included below.)

Probe	Length (kb)	Calculated Hydrolysis Time (min)
Ers1	0.759	49
Kn1	0.300	30
Adc1	0.768	49
BBTI	0.658	46
Pectin lyase	0.683	47

$$t = \frac{L_i - L_f}{0.11 \times L_i \times L_f}$$

L_i = initial length (in kb)

Lf = final length (in kb)

dehydration with a graded EtOH series each for 1.5 min (0.85% NaCl followed by 30%, 50%, 70%, 80%, 90%, 95%, 100% EtOH).

Hybridization and incubations with antibody and detection solution were done by placing two slides together (normal sibling + *Pt1*/+ sibling), face to face, with 250 µl of the corresponding solution. To make each probe solution, 4 µl RNA probe was added to 46 µl 50% formamide (for each slide pair) and heated for 2 min at 80°C before chilling on ice. For each slide pair, the hybridization solution was made with 30.2 µl in situ salts, 100 µl deionized formamide, 50 µl dextran sulfate (that was preheated to 80°C to dispense), 5 µl 50x denhardt's solution, 2.5 µl yeast tRNA, and 17.5 µl nuclease-free water. The hybridization solution and probe solutions were added together (200 µl and 50 µl respectively). The hybridization pairs were incubated overnight at 55°C.

The next day, the slides were washed twice in 0.2X SSC (5 ml 20x SSC, 495 ml ddH_2O) at 55°C for 30 min each and twice in NTE (0.5M NaCl, 10mM Tris, and 1 mM EDTA) at 37°C for 5 min each. RNase treatment (100 µl RNase in 50 ml NTE) for 30 min at 37°C was followed by two NTE washes for 5 min and one 0.2X SSC wash for 60 min at 55°C. Slides were incubated in blocking solution (0.5g Roche blocking reagent, 5 ml 1M Tris HCl ph7.5, 1.5 ml 5M NaCl, 43.5 ml ddH_2O) for 45 min. Detection was performed by incubating the slides with Anti-DIG antibody (Roche diagnostics) diluted 1/4000 in blocking solution (1 µl anti-dig fragments diluted in 4000 µl blocking reagent described above) for 75 min in the dark. Slides were washed at room temperature with buffer A (7l.5 ml 5M NaCl, 25 ml 1M Tris pH 7.5, 216.75ml H_2O, 2.5 g bovine serum albumin) for 15 min four times and with detection buffer (10 ml 1M Tris pH 9.5, 2 ml 5M NaCl, 88 ml H_2O) once for 10 min. Final detection was performed by adding a solution of nitro-blue tetrazolium chloride and 5-bromo-4-chloro-3'-indolyphosphate

(1 tablet dissolved in 10 ml nuclease-free water; Roche) to slides and incubating at room temperature for 24 to 48 h.

To stop the reaction, slide pairs were separated in ddH_2O and dehydrated with an EtOH series (0.85% NaCl followed by 30% EtOH, 50%, 80%, 90%, 95%, 100%) for 5 s each ending with two 5 s Histoclear washes. Approximately 100 µl Permount and long cover slips were added to slides and dried under a fume hood overnight. Slides were imaged with an Olympus BX-41 compound light microscope using CellSense imaging software.

Immunohistochemistry

Indirect immunofluorescence was performed to characterize the boundary between the upper and lower florets of *Pt1* plants. The sections of normal and *Pt1/+* ears were dewaxed with Histoclear and rehydrated with a graded EtOH series. Slides were blocked in 5% BSA solution for 45 min at room temperature. Primary antibodies LM13 and LM20 (Kerafast ELD010 and ELD003) were diluted 1/10 in 5% BSA/1xPBS. Incubations with antibodies were done by placing two slides together, face to face, with 250 µl of corresponding solution. The slide pairs were incubated overnight in a sealed, humidified slide box at 4°C in the dark. After three washes in 1X PBS for 5 min each, the slides were incubated with secondary antibody (goat anti-rat IgG Alexa Flour488, ThermoFisher Scientific, diluted 1:100 in 5% BSA/1xPBS) in a dark, dry incubator at 20°C for 2 hr 45 min. Slides were washed three times in 1x PBS for 5 min each and incubated with 0.02% Toluidine Blue O for 5 min to reduce autofluorescence. The slides were rinsed twice with 1x PBS and mounted with antifade medium (Hinnant et al., 2017) and a coverslip sealed with nail polish. Slides were imaged with a Zeiss LSM700 laser scanning

microscope. Images were processed in Adobe Photoshop and false colored using the Blue Orange icb look up table in ImageJ (Schneider et al., 2012).

Chapter 3: Results

Testing Polytypic ear1's effect on ethylene sensitivity

We hypothesize that the *Pt1* phenotype is caused by overexpression of the ethylene receptor encoded by *ers1*. Since the ethylene receptors are negative regulators of ethylene signaling, we hypothesize that overexpression of a receptor may lead to ethylene insensitivity. In normal maize plants, treatment with the ethylene precursor, ACC, results in reduced growth, indicating that ethylene represses growth (J. Strable, personal communication). To test if *Pt1* plants are sensitive to ethylene, I carried out germination assays in the presence and absence of ACC.

Our first task for the germination assays was finding the optimal dose for ACC. We performed several germination assays using inbreds in the presence and absence of ACC. Initial attempts were unsuccessful due to the ACC. After obtaining new ACC, we repeated the germination assay with A619, B73, and W22 using 50 and 150 µM ACC. The W22 line showed a strong response to ACC, but other inbreds were more variable. W22 seedlings showed a significant decrease in root length in the presence of 50 µM ACC, but A619 and B73 did not (***Figure 9B***). We also relied on more qualitative phenotypes including root morphology. W22 and B73 roots developed extra root hairs resulting in a "fuzzy" appearance (solid triangles in ***Figure 9A***). In addition, roots did not grow linearly and were often kinked in the presence of ACC (open triangles in ***Figure 9A***). A619 showed no consistent change in root morphology. Therefore, we continued our *Pt1* experiment using B73 introgression lines.

If *Pt1* causes a reduction in ethylene sensitivity, then we expected less response to ACC. Overall, plants grown in the absence of ACC had straighter roots than the plants grown in the presence of ACC (***Figure 10A***). In the presence of 50 µM, normal siblings had significantly

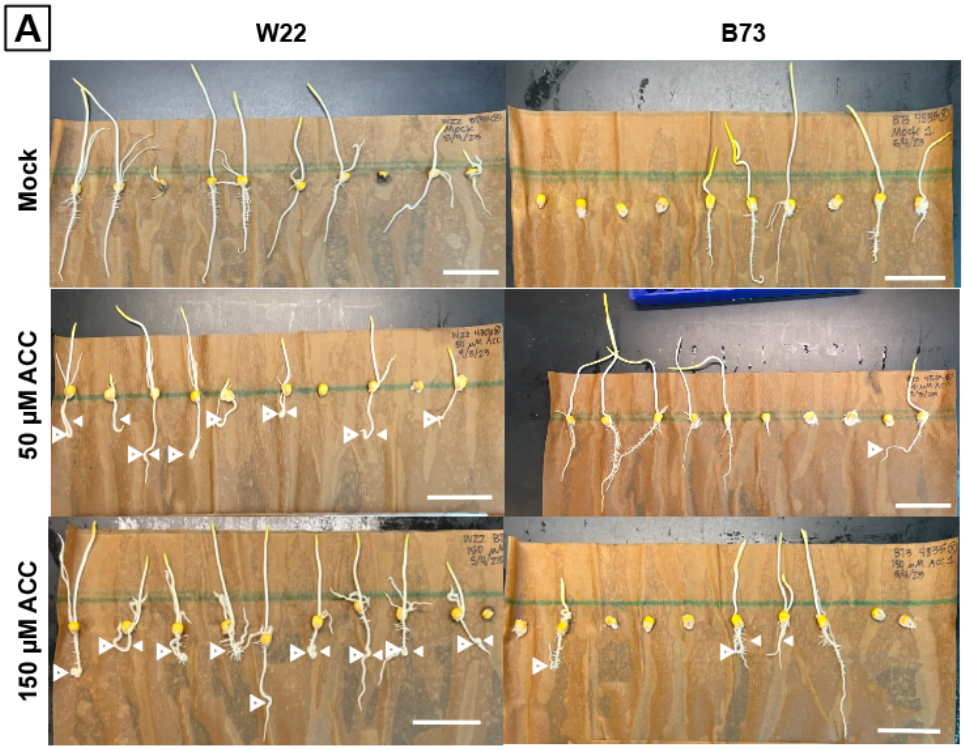
A
W22
B73
Mock
50 µM ACC
150 µM ACC

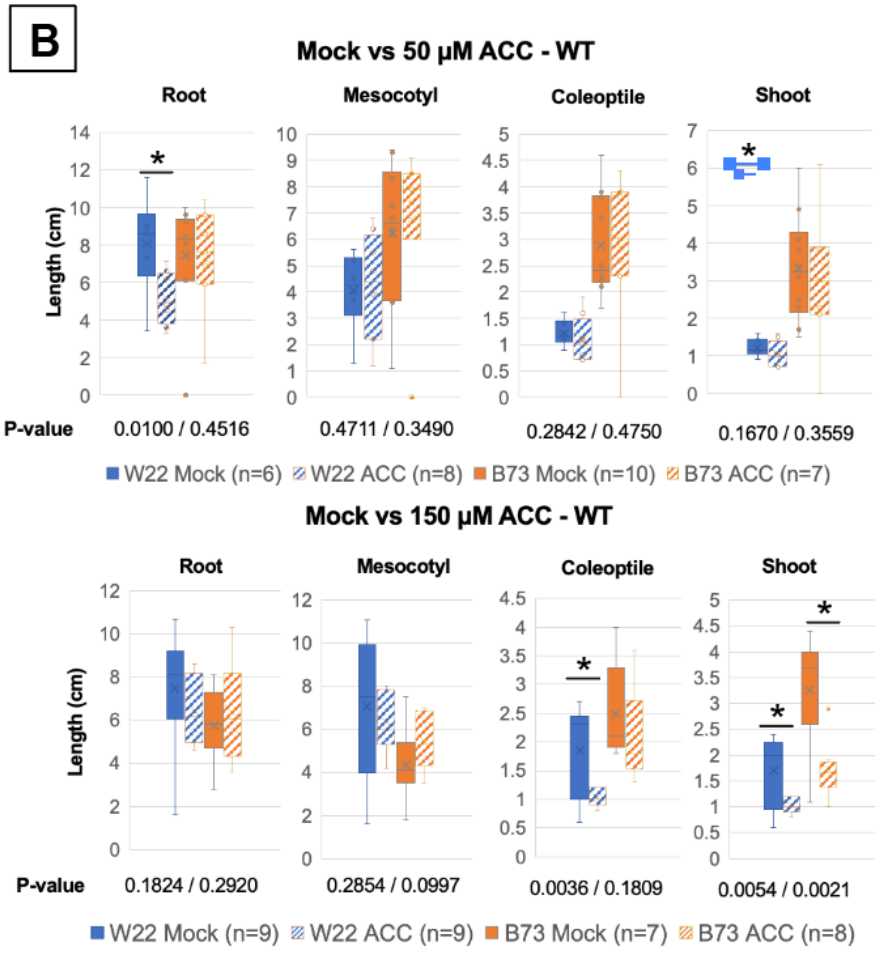
B
Mock vs 50 µM ACC - WT
Root
Mesocotyl
Coleoptile
Shoot
Length (cm)
P-value
0.0100 / 0.4516
0.4711 / 0.3490
0.2842 / 0.4750
0.1670 / 0.3559
W22 Mock (n=6)
W22 ACC (n=8)
B73 Mock (n=10)
B73 ACC (n=7)
Mock vs 150 µM ACC - WT
Root
Mesocotyl
Coleoptile
Shoot
Length (cm)
P-value
0.1824 / 0.2920
0.2854 / 0.0997
0.0036 / 0.1809
0.0054 / 0.0021
W22 Mock (n=9)
W22 ACC (n=9)
B73 Mock (n=7)
B73 ACC (n=8)

Figure 9: Wildtype ACC Assay Results – (A) The mock group (top row) had no ACC in the media, while the ACC group had ACC added to the media – (middle row) 50 μM ACC or (bottom row) 150 μM ACC. N = normal sibling, P = *Pt1*/+ sibling. Scale bar = 5 cm. Solid triangles point to sections of roots that are "fuzzy," while open triangles point to sections of roots that are kinked. (2) Box and whisker plots showing measurements for W22 (blue) and B73 (orange) plants treated with mock solution or ACC solution. The top row compares mock and 50 μM ACC treatments, while the bottom row compares mock and 150 μM ACC treatment. P-values were calculated from one-tailed two-sample T test comparing mock and ACC measurements for each genotype.

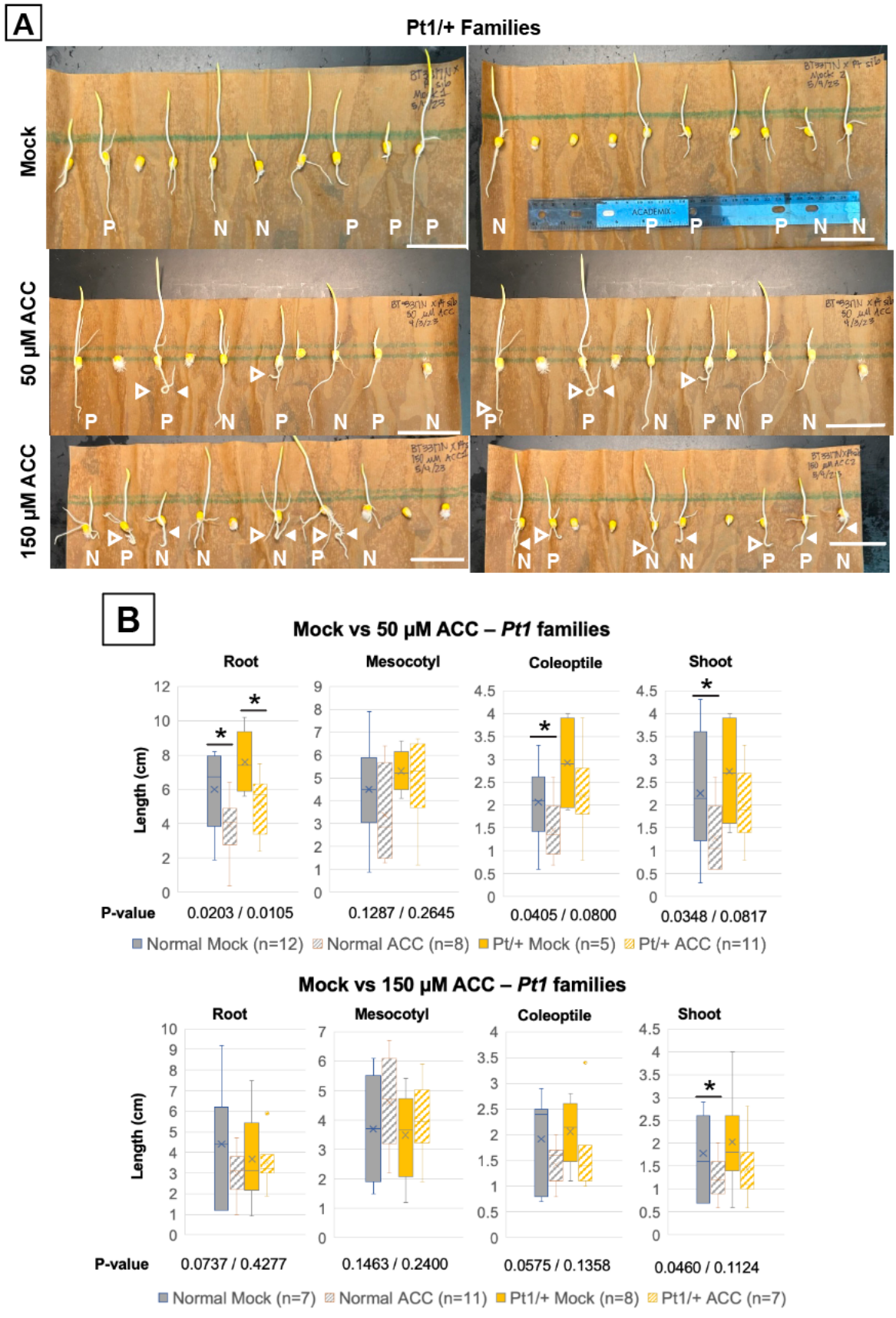
A
Pt1/+ Families
Mock
50 µM ACC
150 µM ACC
B
Mock vs 50 µM ACC – Pt1 families
Root
Mesocotyl
Coleoptile
Shoot
Length (cm)
P-value
0.0203 / 0.0105
0.1287 / 0.2645
0.0405 / 0.0800
0.0348 / 0.0817
Normal Mock (n=12)
Normal ACC (n=8)
Pt/+ Mock (n=5)
Pt/+ ACC (n=11)
Mock vs 150 µM ACC – Pt1 families
Root
Mesocotyl
Coleoptile
Shoot
Length (cm)
P-value
0.0737 / 0.4277
0.1463 / 0.2400
0.0575 / 0.1358
0.0460 / 0.1124
Normal Mock (n=7)
Normal ACC (n=11)
Pt1/+ Mock (n=8)
Pt1/+ ACC (n=7)

Figure 10: ***Polytypic ear1*** **Family ACC Assay Results** – (A) The mock group (top row) had no ACC in the media, while the ACC group had ACC added to the media - (middle row) 50 μM ACC or (bottom row) 150 μM ACC. N denotes a normal sibling, while P denotes a *Pt1/+* sibling. Plants with no letter either did not germinate or had recombinant chromosomes (N at one marker, P at the other). Solid triangles point to sections of roots that are "fuzzy," while open triangles point to sections of roots that are kinked. Scale bar = 5 cm (B) Box and whisker plots showing measurements for normal (gray) and *Pt1* (yellow) plants treated with mock solution or ACC solution. The top row compares mock and 50 μM ACC treatments, while the bottom row compares mock and 150 μM ACC treatment. P-values were calculated from one-tailed two-sample T tests comparing mock and ACC measurements for each genotype.

shorter roots, coleoptiles, and shoots while *Pt1/+* siblings only had significantly shorter roots (***Figure 10B***). In the presence of 150 µM ACC, only normal siblings had significantly shorter shoots compared to no ACC (***Figure 10B***). Pt1/+ siblings had altered root morphology in the presence of 50 and 150 µM ACC, while normal siblings had altered root morphology only in the presence of 150 µM ACC (***Figure 10A***). Based on these results, increasing the ACC concentration did not significantly repress growth in normal plants as expected, but more plants had altered root morphology. It is difficult to draw firm conclusions about *Pt1*'s ACC sensitivity due to inconsistent wildtype results and small sample sizes. Yet *Pt1/+* plants appear to respond to ethylene in root tissue as evidenced by significantly shorter, kinked roots in the presence of ACC. This data suggests that *ers1* may not be overexpressed in *Pt1/+* seedlings.

As an alternative approach to evaluate *ers1* as a candidate gene for *Pt1*, I created an *ers1* RNA probe for RNA *in situ* hybridization. According to RNA-seq results, *ers1* is present in normal and *Pt1/+* siblings at this stage, but *ers1* is upregulated in *Pt1/+* siblings. Unfortunately, I was unable to detect *ers1* transcripts with the *ers1*-specific probe in either normal or *Pt1/+* siblings. Lack of signal with the *ers1* probe could be due to 1) low expression of *ers1, 2)* poor hybridization of probe to the *ers1* mRNA, and 3) technical issues with tissue fixation of the RNA in situ hybridization protocol. I carried out RNA in situ hybridization with the *knotted1* (*Kn1*) probe in parallel as a positive control. *Kn1* is typically expressed in the corpus of spikelet and floral meristems and results in robust staining (Jackson et al., 1994). While I was able to detect *kn1* expression in my tissue, staining was generally weak and not typical of *kn1,* suggesting that the expression patterns of *ers1* may be detectable in different tissue samples (normal and *Pt1/+* siblings).

Characterizing Polytypic ear1's boundary between upper and lower florets

Boundary regions are critical during plant development. During organogenesis, boundary regions are important for correct organ patterning and separation of different activities (Richardson & Hake, 2019). Boundaries become visible microscopically as concave grooves between organs with different developmental fates (Wang et al., 2016). These boundary regions are characterized by low cell division rates and specific gene expression patterns. We have identified a boundary region between the upper and lower florets in developing spikelets that has unique gene expression including *Bowman-Birk-type trypsin inhibitor* (*BBTI;* GRMZM2G114552), *arginine decarboxylase* (GRMZM2G396553) and *pectate lyase homolog* (GRMZM2G131912; Yang et al., 2022). Typically, *BBTI* is expressed at the base of the palea and in discrete domains on the abaxial side of the upper floral meristem but is not expressed in the lower floral meristem. *Pectate lyase* is expressed in discrete domains on the adaxial side of lower floral meristems at the boundary with the upper floral meristem (Yang et al., 2022). *bde* plants, like *Pt1*, have indeterminate floral meristems. In *bde* plants, there is a more widespread expression pattern for *BBTI* (Maynard, 2022). I hypothesized that *Pt1* plants may also have an altered boundary region due to indeterminate floral meristems.

To examine the boundary region between the upper and lower floral meristem in *Pt1,* I attempted RNA *in situ* hybridization. Normal siblings had the characteristic expression patterns for *BBTI* and *pectate lyase* which served as positive controls (***Figure 11***). Both *BBTI* and *pectate lyase* transcripts were also present in a similar domain in *Pt1/+* siblings (***Figure 11***).

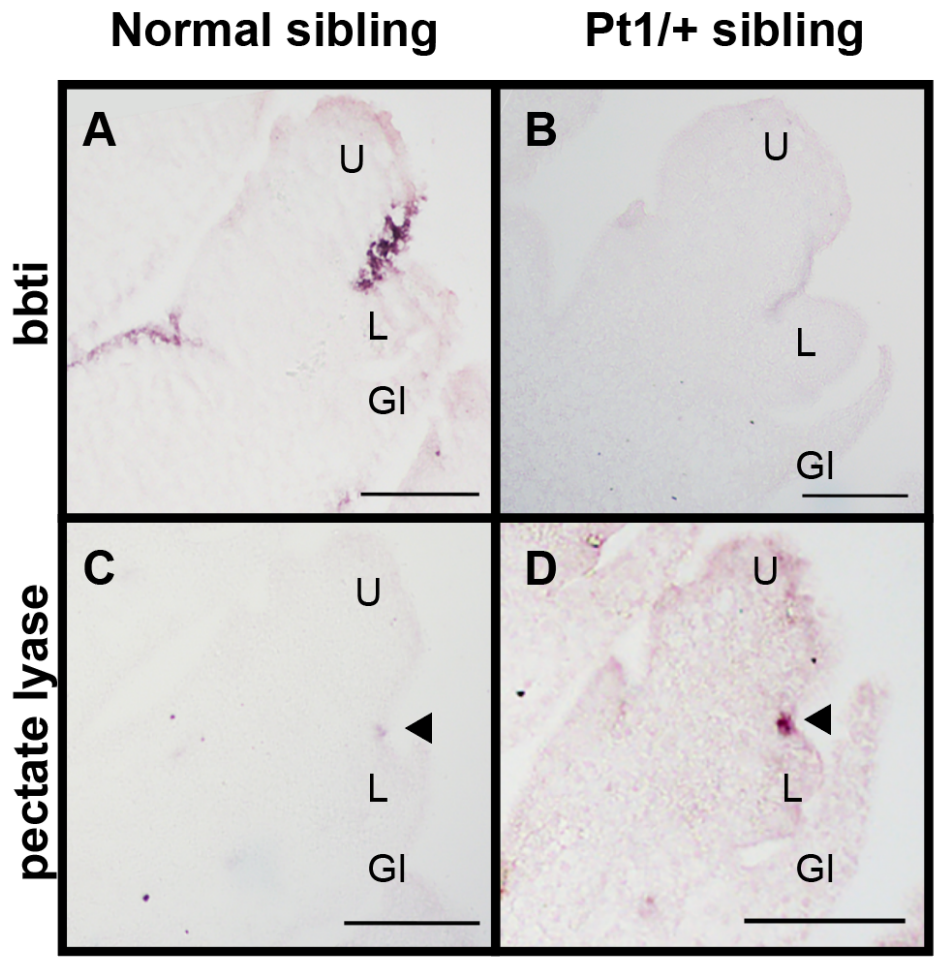

Figure 11: RNA in situs for *bbti* & *pectate lyase* in normal and *Pt1/+* siblings – (Top row) Normal siblings (A) and *Pt1/+* siblings (B) had characteristic expression pattern for *BBTI* (GRMZM2G114552) in a discrete domain of the upper floral meristem. (Bottom row) Normal (C) and *Pt1/+* siblings (C) had characteristic staining for *pectate lyase homolog* (GRMZM2G131912) in a discrete domain on the adaxial side of the lower floral meristem (marked with a solid triangle). U = upper floral meristem; L = lower floral meristem; Gl = glume. Scale bar = 100 μm

Cell wall dynamics also differ between the upper and lower florets and can be altered in floral development mutants. We have specifically focused on pectin, which is a component of the primary cell wall and is important for primordia initiation in Arabidopsis (Peaucelle et al., 2011). Homogalacturonan (HG) is the most abundant pectin and can be fully methylesterified, which is generally associated with rigid cell walls, or demethylesterified, which is associated with more plastic cell walls (Peaucelle et al., 2011). Methylesterified HG has a strong staining pattern on the apical surface of upper floral meristems with reduced or absent staining in lower floral meristems. Methylesterified HG is present in the apical surface of upper floral meristems and the abaxial side of the glume as shown by LM20 staining (Yang et al., 2022). Methylesterified pectin accumulation may be linked to meristem activity. In *bde* mutants, the lower floral meristems are indeterminate, and the lower floret fails to abort. Yet LM20 stains the apical surface of both upper and lower floral meristems in *bde* inflorescences (Maynard, 2022).

We hypothesized that *Pt1* could also have LM20 staining on both floral meristems. Normal (***Figure 12C***) and *Pt1/+* siblings (***Figure 12C'***) had typical LM20 staining on the apical surface of upper floral meristems and the abaxial side of the glume in younger florets. Older florets of normal (***Figure 12D)*** and *Pt1/+* siblings (***Figure 12D'***) also have staining on floral organ primordia. The LM20 staining pattern in *Pt1* is altered in older florets with strong staining on the lower floral meristem (asterisk in ***Figure 12D'***) consistent with *bde's* LM20 staining pattern. The expanded LM20 staining pattern of *bde* and *Pt1/+* plants could be due to indeterminate lower florets showing a link between determinacy and accumulation of methylesterified HG in maize.

RhamnogalacturonanI (RGI) is a pectic epitope that can localize in the boundary region between upper and lower florets. LM13 is a monoclonal antibody that binds to arabinan side

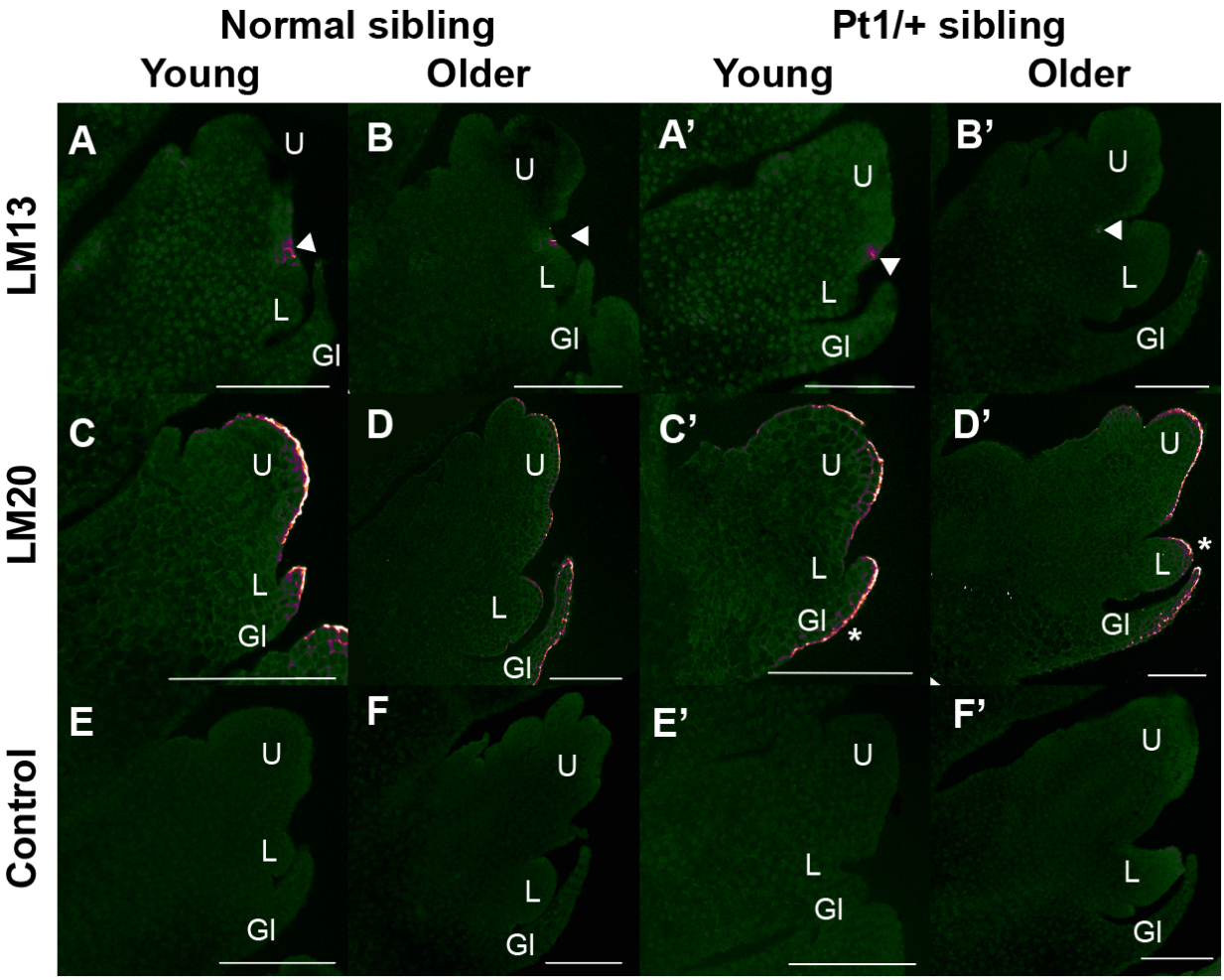

Figure 12: Pectic epitope staining in florets of normal and Pt1/+ siblings – LM13 staining of rhamnogalacturonanI (solid triangle) in young (A) and older (B) florets of normal siblings compared to young (A') and older (B') florets of Pt1/+ siblings. LM20 staining of methylesterified homogalacturonan in young (C) and older (D) florets of normal siblings compared to young (C') and older (D') florets of *Pt1*/+ siblings. An asterisk marks the expanded staining on the abaxial glume of the *Pt1*/+ sibling (D'). Controls processed without primary antibodies in young (E) and older (F) florets of normal siblings compared to young (E') and older (F') florets of and *Pt1*/+ siblings. U = upper floral meristem; L = lower floral meristem; Gl = glume. Scale bar = 100 µm

chains of RGI (Verhertbruggen et al., 2009). B73 inflorescences show strong staining of LM13 in the boundary region between upper and lower floral meristem, while *bde* shows staining extending from the top of the apical surface of initiating lower floral meristems to the top of upper floral meristems and at the top of the developing glume (Maynard, 2022). We hypothesized that *Pt1* would also show an altered LM13 staining pattern consistent with *bde* because both mutants have indeterminate florets. Normal siblings had a typical LM13 staining pattern in a discrete area of the boundary region between upper and lower florets (***Figure 12A-B***, solid triangle). *Pt1/+* siblings did not exhibit an altered boundary region as expected; *Pt1/+* siblings had LM13 staining in a smaller distinct region between upper and lower florets (***Figure 12A'-B'***). Negative controls lacking the primary antibody were included to show the tissue's autofluorescence levels (***Figures 12E-F; 12E'-F'***). Unlike *bde*, *Pt1/+'s* LM13 staining was reduced. The expanded LM13 staining pattern of *bde* plants could be due to additional meristems in the lower floret. The reduced LM13 staining pattern of *Pt1/+* plants could be due to a decrease in accumulation of RGI or technical issues with tissue fixation. Therefore, the accumulation of RGI could be linked to meristematic activity in the lower florets of maize plants.

Chapter 4: Discussion and Future Directions

Polytypic ear1's effect on ethylene sensitivity

This study has shed some light on *Polytypic ear1's* effect on ethylene sensitivity. In the presence of ACC, ethylene's precursor, *Pt1*/+ plants had significantly shorter roots with altered root morphology. Yet it is difficult to draw firm conclusions about *Pt1*'s ACC sensitivity due to inconsistent wildtype results and small sample sizes. The current data suggests that the roots of *Pt1*/+ seedlings are sensitive to ethylene. Yet we know that 8-week old *Pt1*/+ inflorescences overexpress *ers1*. This could be due to a different composition of ethylene receptors in different types of tissue which is true in *Arabidopsis* (Liu and Wen, 2012). The *Pt1* phenotype could be linked to inflorescences insensitive to ethylene as shown by excess floral growth, but more experiments must be done to test this hypothesis.

We know that *ers1* is overexpressed in *Pt1* inflorescences, but we do not know if *ers1* is also overexpressed in other tissues, including seedlings. qRT-PCR could be done with 7-day old normal and *Pt1*/+ seedlings to compare *ers1* expression. If *ers1* is overexpressed in *Pt1*/+ seedlings, the ACC germination assay can be optimized using inbred and *Pt1* seeds with better germination rates. We could also backcross *Pt1*/+ with W22 inbreds that are affected by ACC to get the mutation into a background that exhibits robust ACC responses. Another avenue would be testing ACC's effect on other inbreds we have *Pt1* introgressed with such as Mo17 or A632. If ACC has a reproducible effect on Mo17 or A632, we could repeat the germination assay with *Pt1* introgression lines in these backgrounds in the presence or absence of ACC.

If *ers1* is not overexpressed in *Pt1*/+ seedlings, the next experiment should test ethylene sensitivity in older plants when *ers1* is overexpressed in *Pt1*/+ plants (~8 weeks). Due to lack of time, I was unable to do this experiment. In the future, normal and *Pt1*/+ siblings could be grown

in the presence or absence of 50 and 150 μM ACC in a greenhouse equipped with at least two separate irrigation systems. The flats could be watered with two watering cans, one per treatment group. Once the seedlings are transplanted into pots, the normal and *Pt1*/+ siblings could be split into two groups with separate irrigation systems – one with ACC and the other without ACC added. ACC may cause quantitative changes in tassel or ear development in normal siblings that are not present in *Pt1*/+ siblings. For instance, inflorescences could demonstrate a change in number of spikelets per spikelet pair or number of floral organs or silks per ovule.

In addition to testing ethylene sensitivity directly, we can investigate the expression of *ers1* in developing ears to see if it correlates with the *Pt1* phenotype. The *ers1* probe tested here did not detect any transcripts in either normal or *Pt1*/+ siblings. Another probe may detect transcripts more effectively in another part of the gene. Or a different combination of *ers1* probes could be used successfully. In the future, *Pt1*/+ and normal siblings can be grown and fixed, and using *in situ* solutions at the correct pH, RNA *in situs* can be tested using new *ers1* probes. To draw firmer conclusions, a minimum of three rounds of RNA *in situ*s using at least three different tissue fixations is required.

The *Pt1* phenotype could be caused by a change in the *ers1* coding region. The maize genome is full of chromosomal duplications and rearrangements (Gaut et al., 2000). We can analyze long read PacBio data to investigate the *ers1* genomic region to detect large-scale changes such as chromosomal rearrangements.

Polytypic ear1's boundary between upper and lower florets

We are currently exploring the connection between floral determinacy and the boundary between upper and lower florets. Both *bde* and *Pt1* have indeterminate floral meristems. *bde* has

an altered boundary between upper and lower florets in both *BBTI in situs* and pectic epitope staining. RNA *in situs* revealed the mRNA transcript accumulations of genes expressed in the boundary between upper and lower florets. *Pt1* siblings' accumulation of *BBTI* and *pectate lyase* mRNA transcripts resembled that of normal siblings, but the *in situs* were not as robust as expected. Like *bde*, the LM20 staining pattern of *Pt1/+* plants expanded to include the top apical surface of the lower floret. Unlike *bde,* the LM13 staining pattern of *Pt1/+* plants was reduced to a smaller area between upper and lower florets. Taken together, the data suggests that at least two pectic epitopes are linked with the boundary between upper and lower florets in different ways. LM20 staining was expanded in maize mutants with indeterminate lower floral meristems linking the altered accumulation of methylesterified HG with floral indeterminacy. Yet LM13 staining was expanded in *bde* plants but reduced in *Pt1/+* plants. The LM13 staining could be linked instead to the additional meristems present in *bde* lower florets.

More experiments are needed to draw firmer conclusions about the boundary between *Pt1's* upper and lower florets. We could grow and fix normal and *Pt1/+* siblings to repeat the *BBTI* and *pectate lyase in situs*. In addition to *BBTI* and *pectate lyase in situ*, RNA *in situs* of *arginine decarboxylase1* can be done. We also found that starch accumulates between the upper and lower florets in normal plants (Yang et al., 2022); therefore, iodine staining could help fully characterize the *Pt1* boundary region. If the boundary region is normal in *Pt1*, then a disrupted floret boundary may occur independently from floral meristem determinacy.

Future experiments could include staining for other pectic epitopes. For instance, LM19 binds to demethylesterified HG which has a unique staining pattern in maize flowers. Another experiment could compare the LM13 and LM20 staining patterns for normal and *Pt1/+* tassels. Most of our lab's cell wall staining has been done using plants grown in the B73 background. It

would be interesting to see if *Pt1/+* plants grown in other inbred backgrounds (such as Mo17 or A619) have the same staining patterns as *Pt1/B73* plants. While the characterization of *Pt1* is not yet finished, the future insights gathered about *Pt1* will prove useful to maximize yield and better understand floral development.

References

Alejandra Mandel, M., Gustafson-Brown, C., Savidge, B., & Yanofsky, M. F. (1992). Molecular characterization of the Arabidopsis floral homeotic gene APETALA1. *Nature*, *360*(6401), 273-277.

Ambrose, B. A., Lerner, D. R., Ciceri, P., Padilla, C. M., Yanofsky, M. F., & Schmidt, R. J. (2000). Molecular and genetic analyses of the silky1 gene reveal conservation in floral organ specification between eudicots and monocots. *Molecular Cell, 5*(3), 569-579.

Amoiroglou, A. (2019). Cloning and characterization of the classical maize mutant, Polytypic1. [thesis]. [Greenville (NC)]: East Carolina University. (http://hdl.handle.net/10342/7470.)

Bartlett, M. E., Williams, S. K., Taylor, Z., Deblasio, S., Goldshmidt, A., Hall, D. H., Schmidt, R. J., Jackson, D. P., & Whipplea, C. J. (2015). The maize PI/GLO ortholog Zmm16/sterile tassel silky ear1 interacts with the zygomorphy and sex determination pathways in flower development. *The Plant Cell, 27*(11), 3081-3098.

Becker, A., & Theißen, G. (2003). The major clades of MADS-box genes and their role in the development and evolution of flowering plants. *Molecular Phylogenetics and Evolution, 29*(3), 464-489.

Binder, B. M. (2020). Ethylene signaling in plants. *The Journal of Biological Chemistry*, *295*(22), 7710-7725.

Bomblies, K., Wang, R., Ambrose, B. A., Schmidt, R. J., Meeley, R. B., & Doebley, J. (2003). Duplicate FLORICAULA/LEAFY homologs zfl1 and zfl2 control inflorescence architecture and flower patterning in maize. *Development (Cambridge), 130*(11), 2385-2395.

Bommert, P., Satoh-Nagasawa, N., Jackson, D., & Hirano, H. (2005). Genetics and evolution of inflorescence and flower development in grasses. *Plant and Cell Physiology, 46*(1), 69-78.

Bortiri, E., Jackson, D., & Hake, S. (2006). Advances in maize genomics: the emergence of positional cloning. *Current Opinion in Plant Biology, 9*(2), 164-171.

Cheng, P. C., Greyson, R. I., & Walden, D. B. (1983). Organ initiation and the development of unisexual flowers in the tassel and ear of zea mays. *American Journal of Botany, 70*(3), 450-462.

Draves, M. A., Muench, R. L., Lang, M. G., & Kelley, D. R. (2022). Maize seedling growth and hormone response assays using the rolled towel method. *Current Protocols*, 2, e562.

Favaro, R., Pinyopich, A., Battaglia, R., Kooiker, M., Borghi, L., Ditta, G., ... & Colombo, L. (2003). MADS-box protein complexes control carpel and ovule development in

Arabidopsis. *The Plant Cell*, *15*(11), 2603-2611.

Gallavotti, A., & Whipple, C. J. (2015). Positional cloning in maize (Zea mays subsp. mays, Poaceae). *Applications in Plant Sciences*, *3*(1), apps.1400092.

Gaut, B. S., Le Thierry d'Ennequin, M., Peek, A. S., & Sawkins, M. C. (2000). Maize as a model for the evolution of plant nuclear genomes. *Proceedings of the National Academy of Sciences*, *97*(13), 7008-7015.

Goto, K., & Meyerowitz, E. M. (1994). Function and regulation of the Arabidopsis floral homeotic gene PISTILLATA. *Genes & Development*, *8*(13), 1548-1560.

Gramzow, L., & Theissen, G. (2010). A hitchhiker's guide to the MADS world of plants. *Genome Biology, 11*(6), 214-214.

Jack, T., Brockman, L. L., & Meyerowitz, E. M. (1992). The homeotic gene APETALA3 of Arabidopsis thaliana encodes a MADS box and is expressed in petals and stamens. *Cell*, *68*(4), 683-697.

Jackson, D., Veit, B., & Hake, S. (1994). Expression of maize KNOTTED1 related homeobox genes in the shoot apical meristem predicts patterns of morphogenesis in the vegetative shoot. *Development*, *120*(2), 405-413.

Jofuku, K. D., Den Boer, B. G., Van Montagu, M., & Okamuro, J. K. (1994). Control of Arabidopsis flower and seed development by the homeotic gene APETALA2. *The Plant Cell*, *6*(9), 1211-1225.

Kaplinsky, N. J., & Freeling, M. (2003). Combinatorial control of meristem identity in maize inflorescences. *Development (Cambridge), 130*(6), 1149-1158.

Kaufmann K, Melzer R, Theissen G. (2005). MIKC-type MADS-domain proteins: structural modularity, protein interactions and network evolution in land plants. *Gene*, *347*(2):183-98.

Khan, A. S. (2017). *Flowering plants: Structure and industrial products* (First ed.). John Wiley & Sons, Inc.

Li, M., Zhong, W., Yang, F., & Zhang, Z. (2018). Genetic and molecular mechanisms of quantitative trait loci controlling maize inflorescence architecture. *Plant and Cell Physiology, 59*(3), 448-457.

Li, Q., & Liu, B. (2017). Genetic regulation of maize flower development and sex determination. *Planta, 245*(1), 1-14.

Liu, Q., & Wen, C. K. (2012). Arabidopsis ETR1 and ERS1 differentially repress the ethylene

response in combination with other ethylene receptor genes. *Plant Physiology*, *158*(3), 1193-1207.

Luo, H., Meng, D., Liu, H., Xie, M., Yin, C., Liu, F., Dong, Z., & Jin, W. (2020). Ectopic expression of the transcriptional regulator silky3 causes pleiotropic meristem and sex determination defects in maize inflorescences. *The Plant Cell, 32*(12), 3750-3773.

Maynard, D. (2022). Characterizing the role of pectin in cell wall composition and organ initiation in maize. [thesis]. [Greenville (NC)]: East Carolina University.

Mena, M., Ambrose, B. A., Meeley, R. B., Briggs, S. P., Yanofsky, M. F., & Schmidt, R. J. (1996). Diversification of C-function activity in maize flower development. *Science (American Association for the Advancement of Science), 274*(5292), 1537-1540.

Nelson, O. E., & Postlethwait, S. N. (1954). Variations in Atypical Growth in a Maize Mutant. *American Journal of Botany*, *41*(9), 739–748.

Peaucelle, A., Braybrook, S. A., Le Guillou, L., Bron, E., Kuhlemeier, C., & Höfte, H. (2011). Pectin-induced changes in cell wall mechanics underlie organ initiation in *Arabidopsis*. *Current Biology*, *21*(20), 1720-1726.

Postlethwait S. N., & Nelson, O. E. (1964). Characterization of Development in Maize Through the Use of Mutants. I. The Polytypic (Pt) and Ramosa-1 (ra1) Mutants. *American Journal of Botany*, *51*(3), 238–243.

Richardson, A. E., & Hake, S. (2018;2019;). Drawing a line: Grasses and boundaries. *Plants (Basel), 8*(1), 4.

Riechmann, J. L., Krizek, B. A., & Meyerowitz, E. M. (1996). Dimerization specificity of Arabidopsis MADS domain homeotic proteins APETALA1, APETALA3, PISTILLATA, and AGAMOUS. *Proceedings of the National Academy of Sciences*, *93*(10), 4793-4798.

Strable, J., & Vollbrecht, E. (2019). Maize YABBY genes drooping leaf1 and drooping leaf2 regulate floret development and floral meristem determinacy. *Development (Cambridge), 146*(6)

Tanaka, W., Pautler, M., Jackson, D., & Hirano, H. Y. (2013). Grass meristems II: inflorescence architecture, flower development and meristem fate. *Plant & Cell Physiology*, *54*(3), 313–324.

Theißen, G., Kim, J. T., & Saedler, H. (1996). Classification and phylogeny of the MADS-box multigene family suggest defined roles of MADS-box gene subfamilies in the morphological evolution of eukaryotes. *Journal of Molecular Evolution*, *43*, 484-516.

Theißen, G., Melzer, R., & Ruümpler, F. (2016). MADS-domain transcription factors and the

floral quartet model of flower development: Linking plant development and evolution. *Development (Cambridge), 143*(18), 3259-3271.

Thompson, B. (2014). Chapter Nine - Genetic and Hormonal Regulation of Maize Inflorescence Development. In F. Fornara (Ed.), Advances in Botanical Research (pp. 263–296).

Thompson, B. E., Bartling, L., Whipple, C., Hall, D. H., Sakai, H., Schmidt, R., & Hake, S. (2009). bearded-ear encodes a MADS box transcription factor critical for maize floral development. *The Plant Cell, 21*(9), 2578-2590.

Vanderstraeten, L., Depaepe, T., Bertrand, S., & Van Der Straeten, D. (2019). The ethylene precursor ACC affects early vegetative development independently of ethylene signaling. *Frontiers in Plant Science*, *10*, 1591.

Verhertbruggen, Y., Marcus, S.E., Haeger, A., Ordaz-Ortiz, J.J., Knox, J.P. (2009). An extended set of monoclonal antibodies to pectic homogalacturonan. *Carbohydrate Research, 344* (14),1858 - 1862

Wang, Q., Hasson, A., Rossmann, S., & Theres, K. (2016). Divide et impera: Boundaries shape the plant body and initiate new meristems. *The New Phytologist, 209*(2), 485-498.

Whipple, C. J., Ciceri, P., Padilla, C. M., Ambrose, B. A., Bandong, S. L., & Schmidt, R. J. (2004). Conservation of B-class floral homeotic gene function between maize and *Arabidopsis*. *Development (Cambridge, England)*, *131*(24), 6083–6091.

Yang, H., Nukunya, K., Ding, Q., & Thompson, B. E. (2022). Tissue-specific transcriptomics reveal functional differences in floral development. *Plant Physiology (Bethesda), 188*(2), 1158-1173.

Yanofsky, M. F., Ma, H., Bowman, J. L., Drews, G. N., Feldmann, K. A., & Meyerowitz, E. M. (1990). The protein encoded by the *Arabidopsis* homeotic gene agamous resembles transcription factors. *Nature*, *346*(6279), 35-39.